Effect of Surface Treatment on Diffusion and Domain Formation in Supported Lipid Bilayers

Kalani J. Seu, Anjan P. Pandey, Farzin Haque, Elizabeth A. Proctor, Alexander E. Ribbe, and Jennifer S. Hovis
Department of Chemistry, Purdue University, West Lafayette, Indiana

ABSTRACT Supported lipid bilayers are widely used as model systems due to their robustness. Due to the solid support, the properties of supported lipid bilayers are different from those of freestanding bilayers. In this article, we examine whether different surface treatments affect the properties of supported lipid bilayers. It will be shown that depending on the treatment method, the diffusion of the lipids can be adjusted approximately threefold without altering the composition. Additionally, as the bilayer-support interaction decreases, it becomes easier to form coexisting liquid-ordered and liquid-disordered domains. The physical/chemical alterations that result from the different treatment methods will be discussed.

INTRODUCTION

Supported lipid bilayers are useful model systems for investigating membrane mediated processes, as they maintain the basic structural and dynamic properties of free bilayers (1). They can be formed by vesicle fusion or by the Langmuir-Blodgett (LB)/Langmuir-Schäfer (LS) technique. In either case, an ~0.5- to 1.5-nm-thick water layer is trapped between the bilayer and the support (2–6). The lipids are held close to the surface via hydration, electrostatic, steric, and van der Waals forces (7). The coupling of the bilayer to the solid support affects the membrane properties; the lipids diffuse approximately fivefold more slowly (8) and domains do not easily form (9). In this article, it will be shown that the coupling can be tuned by altering the treatment of the solid support, independent of lipid composition.

Supported lipid bilayers form on a variety of different surfaces, including oxidized gold (10), polymers (11), self-assembled monolayers (12), titanium dioxide (13), oxidized poly(dimethylsiloxane) (PDMS) (14,15), and solid silica surfaces, including mica (16), quartz (2,17), and glass (18). Glass surfaces tend to be the substrate of choice, especially for microscopy. A variety of different treatment methods are used on the glass substrates before bilayers are formed. Typically the substrates are first soaked in a detergent solution to remove silica dust and any organic material, then the substrates are more aggressively treated using a variety of different techniques, including baking (2,19) and chemical etching (e.g., piranha etching) (20). These treatments will affect the physical/chemical properties of the substrate and, consequently, the bilayer-support coupling.

To determine how sensitive the bilayer-support interaction is to treatment method, we examined: 1), the diffusion of lipids in bilayers on differently treated supports; and 2), the effect that treatment method has on the ability to form coexisting liquid-ordered (l_o) and liquid-disordered (l_d) domains. Over the range of surface treatments examined, the lipid diffusion, of the same composition, could be modulated approximately threefold. From the diffusion coefficient, the frictional coefficients were determined for each treatment method. On the surface that gave rise to the fastest diffusion and lowest frictional coefficient, it was possible to form coexisting l_o/l_d domains. To our knowledge, this is the first time large circular l_o domains have been observed on lipid bilayers on glass supports made via vesicle fusion. As will be discussed, by paying attention to how the support is treated it is possible to significantly ameliorate the effect of the support.

EXPERIMENTAL SECTION

Materials

1,2-dioleoyl-*sn*-glycero-3-phosphocholine (DOPC), 1,2-dipalmitoyl-*sn*-glycero-3-phosphocholine (DPPC), cholesterol, and 1-palmitoyl-2-[6-[(7-nitro-2-1,3-benzoxadiazol-4-yl)amino]hexanoyl]-*sn*-glycero-3-phosphocholine (NBD-PC) were purchased from Avanti Polar Lipids (Alabaster, AL). *N*-(Texas Red sulfonyl)-1,2-dihexadecanoyl-*sn*-glycero-3-phosphoethanolamine(TR-DHPE) and CoverWell perfusion chamber gaskets were purchased from Invitrogen-Molecular Probes (Eugene, OR). Glass slides, 22 × 30 #1.5 were purchased from Fisher Scientific (Waltham, MA). ICN 7X detergent was purchased from ICN (Costa Mesa, CA).

Vesicle preparation

Appropriate mixtures of lipids in chloroform were dried under N_2(g) and placed under vacuum for 1 h. Large unilamellar vesicles (LUVs) were formed by reconstituting the lipid film in 18 MΩ-cm water and extruding through a polycarbonate membrane with 50-nm pores a minimum of 21 times. The resulting LUVs were centrifuged at 14,000 rpm for 5 min (MiniSpin Plus, Eppendorf, Melville, NY).

Substrate preparation

Solid glass supports were detergent cleaned by washing in a dilute solution of ICN 7X detergent for at least 10 min, rinsed excessively in 18 MΩ-cm

Submitted October 17, 2006, and accepted for publication December 27, 2006.

Address reprint requests to Jennifer S. Hovis, Dept. of Chemistry, Purdue University, West Lafayette, IN 47907-2018. Tel.: 765-494-4115; Fax: 765-494-0239. E-mail: jhovis@purdue.edu.

0006-3495/07/04/2445/06 $2.00

doi: 10.1529/biophysj.106.099721

water, and dried under a stream of N_2(g) before any additional surface treatment. Annealed glass slides were baked at 450°C for 4 h; the slides were used within 1 h. Piranha-etched glass slides were treated for varying times (5, 20, 40, and 60 min) in a solution of 4:1 (v/v) concentrated sulfuric acid (H_2SO_4) and 30% hydrogen peroxide (H_2O_2), rinsed excessively in 18 MΩ-cm water, and dried under a stream of N_2(g); the slides were used within a few minutes after treatment.

Supported lipid bilayers

Bilayers were formed by vesicle fusion on glass surfaces (18,19). Samples were sandwiched using a coverslip, placed on a homebuilt Delrin sample holder, and kept fully hydrated, using 18 MΩ-cm water, during analysis. Bilayers were imaged using a Nikon TE2000-U fluorescence microscope equipped with a 40× or 100× oil immersion objective, NBD filter sets (Chroma Technology, Bellows Falls, VT) and a Cascade 650 CCD camera (Photometrics, Roper Scientific, Trenton, NJ).

Fluorescence recovery after photobleaching (FRAP)

The FRAP measurements are discussed in detail elsewhere (21). Briefly, a Nikon TE2000-U fluorescence microscope equipped with a 40× oil immersion objective, an NBD filter set (Chroma Technology), and a silicon avalanche photodiode. A single photon counting module (SPCM-AQR-16-FC, PerkinElmer, Vaudreuil, Quebec) was used to focus, collect, and count the emitted fluorescence. A 25-mW Argon ion laser (488 nm, Melles Griot, Carlsbad, CA) was used to both bleach and monitor the lipid bilayer. The bilayers were bleached to background levels (bleach spot radius was 10.6 μm) in 1 s. To reduce further photobleaching of the fluorophore during the recovery period, the laser intensity was reduced 100,000-fold using a 5× (focal transmission of 1×10^5) neutral density filter (NE50B, Thorlabs, Newton, NJ). A LabVIEW program was used to acquire the counts from the avalanche photodiode, control the filter wheel, and trigger the shutter (Uniblitz, Rochester, NY). The fitting of FRAP data to obtain a diffusion coefficient has been discussed in detail elsewhere (22,23). All experiments were conducted at 22°C and the percent fluorescent recovery measured for all experiments was ≥95%.

X-ray photoelectron spectroscopy (XPS)

XPS data were obtained by a Kratos Ultra DLD spectrometer (Manchester, UK) using monochromatic Al K alpha radiation (1486.58 eV). The narrow-region spectra were collected at fixed analyzer pass energy of 20 eV, respectively. A commercial Kratos charge neutralizer was used to achieve a resolution of 1.0–1.2 eV.

Atomic force microscopy (AFM)

AFM measurements were carried out on a Veeco/Di Multimode AFM in tapping mode using oxide sharpened silicon tips (Micromash/NSC15) having a nominal tip radius of <10 nm and a typical resonance frequency of 300–340 KHz. All measurements were done under ambient conditions. The root mean-square (RMS) of height deviations of the individual samples was determined using the provided analysis software (RMS $= \sqrt{(\sum Z_i^2/N)}$, where Z_i are the z- or height values of the respective pixels and N the overall number of pixels). Since the tip radius is in the range of 10 nm, convolution effects have to be considered when interpreting the absolute RMS values of a single image scan. Since we systematically apply the same tip convolution error to each measurement, the comparison of the various samples is reasonable, and the observed trend in RMS change is legitimate.

RESULTS

Effect of surface treatment on diffusion

The choice of solid support treatment has not been well articulated and seems to have more to do with group history and ease of use. Herein it will be shown that the surface treatment has a large effect on lipid fluidity, altering diffusion by approximately threefold. Diffusion coefficients were determined using FRAP. Pioneered by Axelrod et al. (22) and reassessed by Soumpasis (23), methods for calculating the diffusion coefficients of recovering fluorescent molecules into a circular bleached region have been well developed. The recovery data is fit to the solution of the differential equation for lateral transport of a molecule undergoing Brownian motion, using the method of Soumpasis (23):

$$f(t) = e^{(-2\tau_D/t)}[I_o(2\tau_D/t) + I_1(2\tau_D/t)], \quad (1)$$

where τ_D is the characteristic diffusion time and I_0 and I_1 are modified Bessel functions. The diffusion coefficient can then be determined from τ_D using:

$$D = \frac{w^2}{4\tau_D}, \quad (2)$$

where w is the radius of the circular bleach beam and the fluorescence recovery is assumed to be complete.

A significant problem in acquiring FRAP data is eliminating unwanted photobleaching while monitoring the fluorescence. To resolve this issue, the laser power used for monitoring is attenuated to 250 nW, a 100,000-fold decrease compared to the 25-mW bleach laser power. Fig. 1 shows a

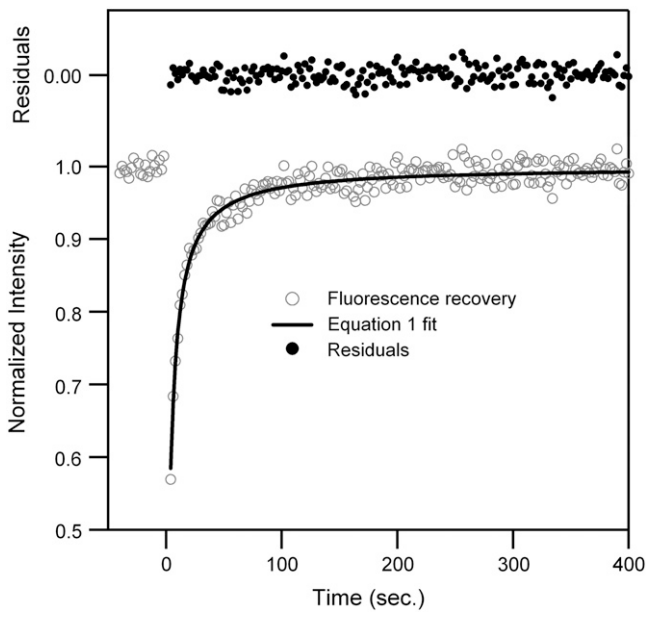

FIGURE 1 Typical FRAP recovery data for a DOPC supported lipid bilayer containing 0.5 mol % NBD-PC with a least-squares fit to Eq. 1. Residuals for the fit to Eq. 1 are at the top of the graph.

typical FRAP recovery curve for a DOPC bilayer with 0.5 mol % NBD-PC, along with a least-squares fit to Eq. 1. In the upper part of Fig. 1 is a plot of the fit residuals. Prebleach data points (time <0) are averaged and used to normalize the recovery data and determine the overall percent recovery. All FRAP data reported have recoveries $\geq$95%. Multiple (minimum of four) FRAP experiments are run on a single lipid bilayer in the same location, and then repeated on a minimum of four different samples. Diffusion values from a single lipid bilayer are averaged and then weighted-averaged with the results of their replicates. This repeated interrogation provides diffusion coefficients containing anywhere from 8 to 16 individual FRAP measurements, with some measurements being rejected based on χ^2 values from the fitted function (21).

The effect that several different treatment methods have on the diffusion coefficient of DOPC bilayers, labeled with 0.5 mol % NBD-PC, can be seen in Fig. 2. In all cases, the slides were placed in warm dilute ICN 7X detergent for 10 min and then rinsed extensively. Further treatment consisted of baking at 450°C for 4 h or piranha etching (4:1 (v/v) concentrated sulfuric acid and 30% hydrogen peroxide) for varying amounts of time. Over the range of treatment methods an approximately threefold change in the diffusion coefficient is observed, with lipids on the baked slides moving the slowest and those on the 5-min-etched slides moving the fastest.

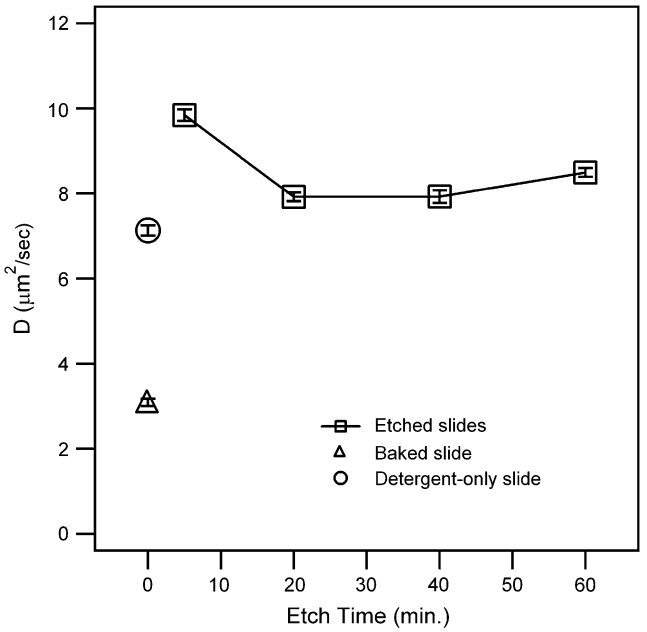

FIGURE 2 Diffusion coefficients of DOPC supported lipid bilayers, containing 0.5 mol % NBD-PC on solid glass supports, plotted as a function of piranha-etched surface treatment time (*open squares*). Plotted at $t = 0$ are the diffusion coefficients of supported lipid bilayers on baked slides (*open triangle*) and on detergent-only slides (*open circle*).

Effect of surface treatment on domain formation

Domains form easily in giant unilamellar vesicles. They are observed to move and, in the case of liquid-ordered domains, merge with one another (24,25). In contrast, domains form much less readily in bilayers on solid supports (9,26,27) and the thermal history of the sample matters; to form gel phase domains on mica, the bilayer needs to be heated above the phase transition temperature (T_m) and cooled slowly back down (26,27). Given that treatment method affects the diffusion, we wanted to examine whether it has a concomitant effect on the ability to form l_o domains.

Bilayers containing DOPC/DPPC/cholesterol/TR-DHPE mixtures that are known to form l_o domains at room temperature (25) were formed on both etched and baked slides. Domains visible by epifluorescence microscopy were observed more frequently in bilayers on etched slides (~67%) than in bilayers on baked slides (~50%). In most cases, domains were only visible if the samples were heated above the T_m and cooled back down to room temperature; only a small percentage of cases (~5%) showed observable domains on the etched slides without heating. The statistics on domain formation were obtained from a minimum of 35 individual samples. In general, our ability to form domains on the 5-min-etched slides was only slightly better than on the slides etched for longer times, so to increase the sample size, the etched samples were clustered together. Fig. 3 shows a bilayer consisting of 2:1 DOPC/DPPC with 15 mol % cholesterol, 0.1 mol % TR-DHPE mixture, on a piranha-etched glass slide, after being heated at 60°C for 1 h. The l_o regions are dark in appearance due to the preferential

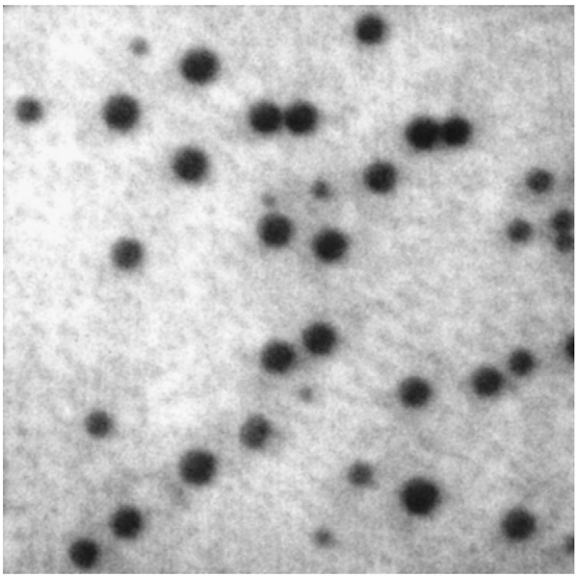

FIGURE 3 Epifluorescence image of a supported lipid bilayer containing 2:1 DOPC/DPPC with 15 mol % cholesterol and 0.1 mol % TR-DHPE on a piranha-etched glass slide, after heating at 60°C for 1 h. The image is 35 μm $\times$ 35 μm and was acquired at room temperature.

separation of the TR-DHPE into the l_d regions (25). Closer analysis of the l_o regions shows that not all of the TR-DHPE has depleted out. To confirm that the domains were l_o, as opposed to defects or gel-phase domains, they were photobleached, and a fast recovery was observed. Unlike in giant unilamellar vesicles, the domains observed on solid supports were not mobile.

Effect of surface treatment on chemical/physical properties of the surface

Both baking and piranha etching further clean the substrate surface, removing dirt/dust and organic material. Baking at 450°C disrupts the hydrogen-bonded surface silanol network, resulting in an increase in isolated silanol groups surrounded by siloxanes (28). Though the surface still remains hydrophilic after baking, the decrease in the number of surface silanols causes an overall reduction in surface hydrophilicity. Piranha etch, on the other hand, is a strong oxidizer and will hydroxylate the surface by increasing silanol groups and Si-O^- species on the glass support, making the surface more hydrophilic.

It is obvious, when working with the different slides, that the etched slides are more hydrophilic. However, it is not possible to quantitatively determine the difference, as all of the treatment methods render the surfaces too hydrophilic for contact-angle measurements. With XPS, it is possible to examine the oxidation state of the silicon atoms at and near the surface. The Si(2p) peak is shown in Fig. 4 for baked, 5-min-etched, and 20-min-etched slides; the lower the binding energy, the lower the oxidation state of the silicon (29). The baked slide is shifted to lower binding energies than either of the etched slides, in agreement with the statement that baking reduces the surface silanol groups. The O(1s) peak has also been examined, and again the etched slides are similar and differ from the baked slide; however, interpretation is complicated due to the advantageous carbon.

To examine whether etching induced significant roughening of the surfaces, AFM was used. Fig. 5 shows AFM images and line scans from five different samples; a baked slide and four slides that have been piranha-etched for varying amounts of time. The topography of the baked and 5-min-etched slides appears to be fairly similar, whereas a noticeable roughening can be observed as the etch time is increased. As it is difficult to gauge the differences in roughness strictly from the AFM images and line scans, Table 1 gives the RMS values determined over a 1 μm $\times$ 1 μm area of the slides (these values come from two independent measurements). The RMS values confirm the observation that surface roughness increases with longer etch times, with the largest topographical difference between the baked slides and the 40- or 60-min-etched slides. There was no statistical difference between the RMS values of detergent-cleaned, but otherwise untreated, slides and the baked slides. Though there is a measurable difference in surface topography with etching, the roughening of the support surface is not significant enough to disrupt supported lipid bilayer formation, and the bilayer should have no problem contouring to the surface (30–32). That the drop in diffusion between the 5-min and 60-min-etched slides is an artifact due to the increased surface area can be discounted, as the change in area is miniscule.

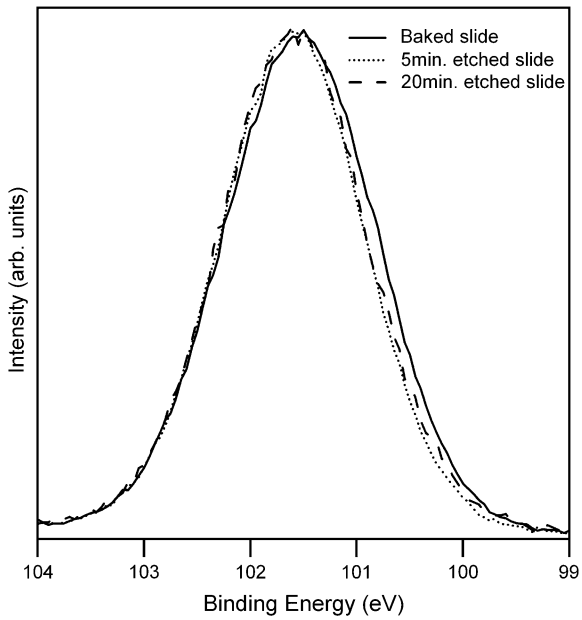

FIGURE 4 X-ray photoelectron spectra of the Si(2p) region. Three treatment methods were examined: baked, 5-min etched, and 20-min etched.

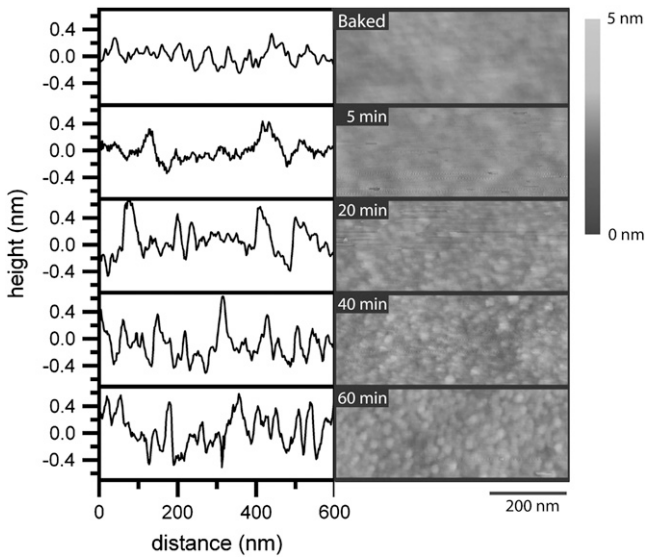

FIGURE 5 AFM line scans and corresponding images of a baked slide and slides etched for 5, 20, 40, and 60 min. Note: the height scale has been emphasized to help visualize the small change in surface undulations.

TABLE 1 Surface roughness of glass after various treatments

Treatment	RMS (nm)	% Increase from flat surface
Detergent-only	0.13	0.4
Baked	0.13	0.4
5-min etch	0.15	0.6
20-min etch	0.22	1.8
40-min etch	0.27	2.4
60-min etch	0.26	2.5

RMS values indicate roughness. Percent increase in surface area is indicated in final column. RMS values were obtained from a 1 μm $\times$ 1 μm area, as described in the Experimental section.

DISCUSSION

When working with supported lipid bilayers, it is important that their properties mimic the properties of freestanding bilayers as closely as possible. The results presented here show that, to this end, the choice of treatment method is nontrivial. As an aside, we note that these results may have another practical implication. There are instances where the question of the effect of fluidity on biological processes arises. This question is difficult to address experimentally, since to alter the diffusion it is necessary to alter the composition. The results presented in this article provide a method to change lipid diffusion without altering the composition. Consequently, they may prove to be invaluable for examining a variety of biological processes.

In the strong coupling limit, diffusion can be related to the frictional coefficient, b_s (33), as follows:

$$D = \frac{k_B T}{\pi b_s a_p^2}, \tag{3}$$

where a_p is the van der Waals radius of the diffusant (34). For each treatment method, the frictional coefficient is given, along with the diffusion coefficient, in Table 2. It is assumed that a_p remains constant; to check that this is the case, we examined the initial counts in the FRAP experiments. If a_p changes, then the number of labeled lipids within a specific region will vary. As a result, the initial counts in the FRAP experiments would be sensitive to this intensity difference. There is some error in our ability to measure the NBD-PC when mixed with the DOPC; consequently, each vesicle sample does not contain exactly 0.5 mol % NBD-PC. Within this error ($\pm$15%), the initial counts did not vary from one treatment method to another, allowing us to conclude that a_p remains constant. The frictional coefficient was observed to vary from 6×10^7 to 1.8×10^8 dyne s/cm^3. In comparison, the frictional coefficient was observed to vary from 1×10^6 to 6.8×10^9 dyne s/cm^3 when polymer supports were used (34). By exposing the surface to 4:1 (v/v) concentrated sulfuric acid and 30% hydrogen peroxide for 5 min, it is possible to reduce the frictional coupling to levels close to that which can be achieved with polymer supports.

TABLE 2 Diffusion and frictional coefficient after various treatments

Treatment	Diffusion (μm^2/s)	Frictional coefficient (dyn s/cm^3)
Detergent-only	7.1 $\pm$ 0.1	7.9×10^7
Baked	3.1 $\pm$ 0.1	1.8×10^8
5 min etch	9.8 $\pm$ 0.1	5.7×10^7
20 min etch	7.9 $\pm$ 0.1	7.1×10^7
40 min etch	7.9 $\pm$ 0.1	7.1×10^7
60 min etch	8.5 $\pm$ 0.1	6.6×10^7

To calculate the frictional coefficient, a temperature of 23°C and a particle radius of 4.8 Å were assumed for DOPC (36).

The frictional coefficient can be related to the viscosity of the water layer:

$$b_s = \frac{\eta_w}{h}, \tag{4}$$

where h is the thickness of the water layer (33). On glass, it is impossible to determine the water-layer thickness. Nevertheless, three possibilities can be contemplated: 1), Assuming a thickness of 1 nm, the viscosity is found to vary from 5.7 Poise on the 5-min-etched slides to 18 poise on the baked slides; these values are ~1000-fold greater than the viscosity of bulk water (0.01 poise). 2), If the viscosity is instead fixed, at 10 poise, then the height varies from 1.7 nm on the 5-min-etched sides to 0.5 nm on the baked slides; very close to the reported distance of the bilayer from the surface, 0.5–1.5 nm (2–6). 3), The height varies, but in a manner opposite to that in the previous case (the bilayers are closer on the etched slides than on the baked slides); in this case, the viscosity of the water layer is less on the baked slides than on the etched slides (baked, 9.1 poise, assuming 1.7 nm; etched, 9.7 poise, assuming 0.5 nm).

Previous work examining confined water layers shows that the viscosity of the water layer is greater when the layer is trapped between two hydrophilic surfaces than when it is trapped between a hydrophilic surface and a hydrophobic surface (35). Simulations show that at short separation, the number of hydrogen-bond contacts to the surface is greater in the case of the water confined between the two hydrophilic surfaces (35). These results indicate that the viscosity of the water layer trapped between the bilayer and the slide should be greater when the slides are etched than when they are baked. This suggests that the third possibility above might be representative of the effect that treatment has on the water viscosity. Work is ongoing to explore the structure of the water layer further. Regardless of the molecular-level details, the basic observations in this article are of great importance to anyone working with supported lipid bilayers.

CONCLUSION

The effects that several different treatment methods have on supported bilayer properties were examined. Over the range of treatments—baking, detergent-only, and piranha etching—the lipid diffusion was observed to change approximately

threefold. This change in diffusion coefficient was independent of composition, as the lipid mixture was held constant. The fastest diffusion was observed on the surfaces that were etched for 5 min. These surfaces also gave the lowest frictional coefficient. It was also observed that the surfaces that gave rise to the fastest diffusion also gave rise to the greatest probability of observing liquid-ordered domains.

The authors thank Dr. D. Zemlyanov of the Surface Analysis Laboratory, Birck Nanotechnology Center, Purdue University, for assistance with the x-ray photoelectron spectroscopy experiments.

J.S.H. is a recipient of a Career Award in the Biomedical Sciences from the Burroughs Wellcome Fund.

REFERENCES

1. Sackmann, E. 1996. Supported membranes: scientific and practical applications. *Science*. 271:43–48.
2. Kim, J., G. Kim, and P. S. Cremer. 2001. Investigations of water structure at the solid/liquid interface in the presence of supported lipid bilayers by vibrational sSum frequency spectroscopy. *Langmuir*. 17: 7255–7260.
3. Bayerl, T. M., and M. Bloom. 1990. Physical properties of single phospholipid bilayers adsorbed to micro glass beads: a new vesicular model system studied by 2H-nuclear magnetic resonance. *Biophys. J*. 58:357–362.
4. Johnson, S. J., T. M. Bayerl, D. C. McDermott, G. W. Adam, A. R. Rennie, R. K. Thomas, and E. Sackmann. 1991. Structure of an adsorbed dimyristoylphosphatidylcholine bilayer measured with specular reflection of neutrons. *Biophys. J*. 59:289–294.
5. Koenig, B. W., S. Krueger, W. J. Orts, C. F. Majkrzak, N. F. Berk, J. V. Silverton, and K. Gawrisch. 2001. Neutron reflectivity and atomic force microscopy studies oa a lipid bilayer in water adsorbed to the surface of a silicon single crystal. *Langmuir*. 12:1343–1350.
6. Mou, J., J. Yang, and Z. Shao. 1994. Tris(hydroxymethyl)aminomethane ($C_4H_{11}NO_3$) induced a ripple phase in supported unilamellar phospholipid bilayers. *Biochemistry*. 33:4439–4443.
7. Israelachvili, J. 1992. Intermolecular and Surface Forces. Academic Press, New York.
8. Sonnleitner, A., G. J. Schutz, and T. Schmidt. 1999. Free Brownian motion of individual lipid molecules in biomembranes. *Biophys. J*. 77: 2638–2642.
9. Stottrup, B. L., S. L. Veatch, and S. L. Keller. 2004. Nonequilibrium behavior in supported lipid membranes containing cholesterol. *Biophys. J*. 86:2942–2950.
10. Keller, C. A., and B. Kasemo. 1998. Surface specific kinetics of lipid vesicle adsorption measured with a quartz crystal microbalance. *Biophys. J*. 75:1397–1402.
11. Jenkins, A. T. A., J. Hu, Y. Z. Wang, S. Schiller, R. Foerch, and W. Knoll. 2000. Pulsed plasma deposited maleic anhydride thin films as supports for lipid bilayers. *Langmuir*. 16:6381–6384.
12. Williams, L. M., S. D. Evans, T. M. Flynn, A. Marsh, P. F. Knowles, R. J. Bushby, and N. Boden. 1997. Kinetics of the unrolling of small unilamellar phospholipid vesicles onto self-assembled monolayers. *Langmuir*. 13:751–757.
13. Starr, T. E., and N. L. Thompson. 2000. Formation and characterization of planar phospholipid bilayers supported on TiO2 and SrTiO3 single crystals. *Langmuir*. 16:10301–10308.
14. Lenz, P., C. M. Ajo-Franklin, and S. G. Boxer. 2004. Patterned supported lipid bilayers and monolayers on poly(dimethylsiloxane). *Langmuir*. 20:11092–11099.
15. Hovis, J. S., and S. G. Boxer. 2001. Patterning and composition arrays of supported lipid bilayers by microcontact printing. *Langmuir*. 17: 3400–3405.
16. Yang, J., L. K. Tamm, T. W. Tillack, and Z. Shao. 1993. New approach for atomic force microscopy of membrane proteins: the imaging of cholera toxin. *J. Mol. Biol*. 229:286–290.
17. Kalb, E., S. Frey, and L. K. Tamm. 1992. Formation of supported planar bilayers by fusion of vesicles to supported phospholipid monolayers. *Biochim. Biophys. Acta*. 1103:307–316.
18. Brian, A. A., and H. M. McConnell. 1985. Allogenic stimulation of cytotoxic T cells by supported planar membranes. *Proc. Natl. Acad. Sci. USA*. 81:6159–6163.
19. Cremer, P. S., and S. G. Boxer. 1999. Formation and spreading of lipid bilayers on planar glass supports. *J. Phys. Chem. B*. 103:2554–2559.
20. Hull, M. C., L. R. Cambrea, and J. S. Hovis. 2005. Infrared spectroscopy of fluid lipid bilayers. *Anal. Chem*. 77:6096–6099.
21. Seu, K. J., L. R. Cambrea, R. M. Everly, and J. S. Hovis. 2006. Influence of lipid chemistry on membrane fluidity: tail and headgroup interactions. *Biophys. J*. 91:3727–3735.
22. Axelrod, D., D. E. Koppel, J. Schlessinger, E. Elson, and W. W. Webb. 1976. Mobility measurement by analysis of fluorescence photobleaching recovery kinetics. *Biophys. J*. 16:1055–1069.
23. Soumpasis, D. M. 1983. Theoretical analysis of fluorescence photobleaching recovery experiments. *Biophys. J*. 41:95–97.
24. Korlach, J., P. Schwille, W. W. Webb, and G. W. Feigenson. 1999. Characterization of lipid bilayer phases by confocal microscopy and fluorescence correlation spectroscopy. *Proc. Natl. Acad. Sci. USA*. 96:8461–8466.
25. Veatch, S. L., and S. L. Keller. 2003. Separation of liquid phases in giant vesicles of ternary mixtures of phospholipids and cholesterol. *Biophys. J*. 85:3074–3083.
26. McKiernan, A. E., T. V. Ratto, and M. L. Longo. 2000. Domain growth, shapes, and topology in cationic lipid bilayers on mica by fluorescence and atomic force microscopy. *Biophys. J*. 79:2605–2615.
27. Lin, W.-C., C. D. Blanchette, T. V. Ratto, and M. L. Longo. 2006. Lipid asymmetry in DLPC/DSPC-supported lipid bilayers: a combined AFM and fluorescence microscopy study. *Biophys. J*. 90:228–237.
28. Morrow, B. A., and I. D. Gay. 2000. Infrared and NMR characterization of the silica surface. *In* Adsorption on Silica Surfaces. E. Papirer, editor. John Wiley and Sons, New York.
29. Himpsel, F. J., F. R. Mcfeely, A. Talebibrahimi, J. A. Yarmoff, and G. Hollinger. 1988. Microscopic structure of the SiO2/Si interface. *Phys. Rev. B*. 38:6084–6096.
30. Richter, R. P., and A. Brisson. 2003. Characterization of lipid bilayers and protein assemblies supported on rough surfaces by atomic force microscopy. *Langmuir*. 19:1632–1640.
31. Mornet, S., O. Lambert, E. Duguet, and A. Brisson. 2005. The formation of supported lipid bilayers on silica nanoparticles revealed by cryoelectron microscopy. *Nano Lett*. 5:281–285.
32. Weng, K. C., J. J. R. Stålgren, D. J. Duval, S. H. Risbud, and C. W. Frank. 2004. Fluid biomembranes supported on nanoporous aerogel/xerogel substrates. *Langmuir*. 20:7232–7239.
33. Evans, E., and E. Sackmann. 1988. Translational and rotational drag coefficients for a disk moving in a liquid membrane associated with a rigid substrate. *J. Fluid Mech*. 194:553–561.
34. Kuhner, M., R. Tampe, and E. Sackmann. 1994. Lipid mono- and bilayer supported on polymer films: composite polymer-lipid films on solid substrates. *Biophys. J*. 67:217–226.
35. Major, R. C., J. E. Houston, M. J. McGrath, J. I. Siepmann, and X.-Y. Zhu. 2006. Viscous water meniscus under nanoconfinement. *Phys. Rev. Lett*. 96:177803.
36. Kucerka, N., S. Tristram-Nagle, and J. F. Nagle. 2006. Structure of fully hydrated fluid phase lipid bilayers with monounsaturated chains. *J. Membr. Biol*. 208:193–202.